Mean charge of ions ($5 \leq Z_1 \leq 25$) emerging from aluminum foils

W. N. Lennard, T. E. Jackman, and D. Phillips
Atomic Energy of Canada Limited Research Company, Solid State Science Branch, Chalk River, Ontario, Canada KOJ 1J0

(Received 18 May 1981)

We have determined the mean charge $\bar{q}$ for projectiles $5 \leq Z_1 \leq 25$ exiting thin Al foils at a velocity $v = v_0$. The results are compared with previous data for the same projectiles exiting thin C foils. In the region $Z_i \sim 15$, the differences $\bar{q}(\mathrm{C}) - \bar{q}(\mathrm{Al})$ are observed to be as large as solid-gas differences.

Charge states for ions (Z_1) moving through matter (Z_2) have been of interest for nearly forty years. The review by Betz[1] examined both the experimental and theoretical aspects of charge states in matter and the systematics of charge exchange processes. Owing to the complexity of the capture and loss interactions there is still no theoretical framework which allows calculation of these values with any reasonable precision. There are, however, numerous semiempirical expressions which attempted to describe the early experimental data for projectile mean charges $\bar{q}$ by a monotonically increasing function of Z_1, but independent of Z_2. Betz[1] has noted that for fixed Z_1 $\bar{q}$ determined from sparse solid target data appears to decrease slowly but monotonically with increasing Z_2 for projectile velocities $v \gtrsim 2v_0$. However, no systematic measurements have been made of the target-material dependence of $\bar{q}(Z_2)$ for low-velocity ions.

Lennard *et al.*[2,3] have recently reported measurements of post-foil charge-state distributions for projectiles, $5 \leq Z_1 \leq 26$, emerging at low velocities, $v \sim v_0$, from thin carbon foils. These results demonstrate first that the Z_1 dependence of $\bar{q}$ for low-velocity ions exciting carbon foils is nonmonotonic with Z_1, and second that the structure is not simply correlated with projectile ionization potentials. Because of the unexpected Z_1 dependence found in carbon, $Z_2 = 6$, the dependence of $\bar{q}$ on target material Z_2 would then seem difficult to predict.

In this paper we report the measurement of post-foil charge-state distributions for projectiles, $5 \leq Z_1 \leq 25$, emerging at low velocities from thin aluminum foils ($Z_2 = 13$). The Z_2 value was chosen to be comparable to the value of Z_1 for which a local maximum was observed in $\bar{q}(Z_1)$ in the carbon data.[2] The projectile velocity $v = v_0$ was the same as in the earlier measurements where such a Z_1 structure was pronounced.

The experimental technique has been described in detail previously.[3] For the aluminum measurements the target was surrounded by a 100-K cold shroud in order to avoid buildup of carbon.[4] All aluminum foils had a native oxide on both surfaces corresponding to $1 \pm 0.1\ \mu\mathrm{g\,cm}^{-2}$ of Al_2O_3 as determined by Rutherford backscattering. Measurements made with foils of different thicknesses revealed no change in charge state, i.e., equilibrium was achieved for the thinnest foils used, viz., for 20-$\mu\mathrm{g\,cm}^{-2}$-thick targets. It should be noted that the measured charge-state distributions, although designated $\bar{q}(\mathrm{Al})$, are not characteristic of pure Al but of this Al-Al_2O_3 system. Charge-state distributions were measured for a few different exit velocities from which a value at $v = v_0$ was derived by linear interpolation. In addition, charge-state distributions for carbon foils $\bar{q}(\mathrm{C})$ were also measured in the same "clean" environment and reproduced the earlier results.[3]

The charge-state-distribution results for Al are given in Table I together with $\bar{q}(\mathrm{Al})$ and d, the mean charge and width, respectively, where $d^2 = \sum_q (q - \bar{q})^2 f_q$. The quantity f_q is the fraction of the beam detected in charge state q. The uncertainties are the same as discussed in detail for the carbon foil data and are typically $1-3\,\%$ for $\bar{q}$.[3]

In Fig. 1 we show the $\bar{q}(\mathrm{Al})$ results as a function of Z_1. The carbon data from Ref. 2 are reproduced here together with gas target values ($Z_1 \rightarrow N_2$, O_2) interpolated at $v = v_0$ from data in Ref. 5. We observe that $\bar{q}$ for projectiles emerging from Al foils increases strongly with Z_1 as it does for carbon foils but does not display the pronounced peak that was observed for $\bar{q}(\mathrm{C})$. In fact, the solid-solid difference $\bar{q}(\mathrm{C}) - \bar{q}(\mathrm{Al})$ can amount to

TABLE I. Equilibrium charge fractions (f_q), mean charges ($\bar{q}$), and distribution widths (d) for projectiles exiting a thin, aluminum foil as a function of emergent beam energy (in keV).

Projectile	Energy	$\bar{q}$	d	f_{-1}	f_0	f_1	f_2	f_3	f_4	f_5	f_6	f_7	f_8
$^{11}_{5}B$	253.1	1.028	0.646		0.185	0.613	0.192	0.0102					
	280.7	1.057	0.656		0.175	0.606	0.206	0.0132					
	294.5	1.097	0.668		0.163	0.593	0.227	0.0163					
	308.4	1.121	0.669		0.154	0.592	0.238	0.0175					
$^{12}_{6}C$	269.6	0.990	0.728	0.0081	0.234	0.532	0.214	0.0126					
	293.1	0.990	0.739	0.0086	0.238	0.521	0.218	0.0139					
	321.4	1.062	0.742	0.0068	0.208	0.521	0.246	0.0184					
$^{14}_{7}N$	318.2	1.167	0.785		0.197	0.481	0.280	0.0416					
	348.0	1.200	0.828		0.208	0.441	0.296	0.0556					
	373.8	1.202	0.796		0.190	0.465	0.299	0.0462					
$^{16}_{8}O$	364.5	1.383	0.859	0.0093	0.125	0.435	0.340	0.0887	0.003 20				
	396.4	1.453	0.846	0.0076	0.103	0.427	0.354	0.108					
	428.5	1.528	0.877	0.0072	0.0976	0.390	0.377	0.123	0.005 92				
$^{19}_{9}F$	425.9	1.597	0.932	0.0045	0.115	0.332	0.389	0.146	0.0133				
	467.9	1.722	0.912	0.0039	0.0828	0.308	0.412	0.180	0.0134				
	514.7	1.817	0.924	0.0028	0.0686	0.291	0.407	0.209	0.0221				
$^{20}_{10}Ne$	459.6	1.896	0.929		0.0610	0.276	0.397	0.236	0.0292				
	497.1	1.978	0.925		0.0495	0.254	0.401	0.259	0.0363				
	534.7	2.071	0.921		0.0378	0.234	0.391	0.294	0.0436				
$^{23}_{11}Na$	530.4	2.124	0.878		0.0161	0.227	0.429	0.272	0.0557				
	573.7	2.204	0.893		0.0129	0.206	0.418	0.290	0.0729				
	617.1	2.301	0.883		0.0093	0.174	0.405	0.329	0.0826				
$^{24}_{12}Mg$	537.5	2.296	0.857		0.0076	0.156	0.454	0.298	0.0842				
	593.1	2.408	0.886		0.0063	0.126	0.440	0.318	0.102	0.0082			
	648.8	2.491	0.888		0.0034	0.111	0.415	0.345	0.115	0.0111			

TABLE I. (*Continued.*)

Projectile	Energy	$\bar{q}$	d	f_{-1}	f_0	f_1	f_2	f_3	f_4	f_5	f_6	f_7	f_8
$^{27}_{13}Al$	608.1	2.373	0.936		0.0093	0.166	0.385	0.332	0.0984	0.009 65			
	650.0	2.448	0.935		0.0076	0.143	0.380	0.345	0.114	0.0113			
	692.1	2.502	0.924		0.0057	0.127	0.373	0.363	0.118	0.0134			
	734.2	2.559	0.922		0.0049	0.109	0.369	0.375	0.125	0.0178			
$^{31}_{15}P$	715.9	2.535	1.210		0.0290	0.177	0.306	0.267	0.160	0.0610			
	728.7	2.528	1.200		0.0285	0.172	0.316	0.273	0.150	0.0582	0.002 25		
	772.9	2.569	1.192		0.0280	0.159	0.312	0.280	0.159	0.0618			
	776.0	2.637	1.213		0.0280	0.144	0.303	0.290	0.163	0.0688	0.003 81		
	829.9	2.716	1.210		0.0151	0.146	0.292	0.288	0.180	0.0717	0.007 32		
$^{32}_{16}S$	727.8	2.617	1.235		0.0129	0.171	0.326	0.259	0.152	0.0629	0.0158		
	791.2	2.738	1.262		0.0129	0.150	0.304	0.268	0.167	0.0829	0.0158		
	859.3	2.824	1.259		0.0095	0.132	0.298	0.275	0.179	0.0873	0.0198		
$^{35}_{17}Cl$	781.2	2.681	1.201		0.0144	0.131	0.338	0.290	0.150	0.0584	0.0189		
	866.8	2.827	1.227		0.0098	0.108	0.317	0.301	0.170	0.0696	0.0212	0.003 80	
	952.7	2.990	1.267		0.0067	0.0867	0.293	0.304	0.183	0.0932	0.0249	0.007 83	
$^{40}_{18}Ar$	918.0	2.730	1.148		0.0082	0.117	0.322	0.333	0.148	0.0548	0.0179		
	994.7	2.870	1.140		0.0034	0.0964	0.291	0.346	0.185	0.0565	0.0221		
	1071.6	2.968	1.181		0.0053	0.0826	0.272	0.351	0.188	0.0698	0.0310		
$^{39}_{19}K$	902.1	2.928	1.090		0.0034	0.0724	0.281	0.376	0.188	0.0619	0.0174		
	974.2	3.027	1.114		0.0040	0.0603	0.272	0.346	0.221	0.0797	0.0170		
	1046.3	3.189	1.134		0.0031	0.0427	0.230	0.356	0.257	0.0826	0.0200	0.007 83	
$^{52}_{24}Cr$	1195.9	3.797	1.490		0.0080	0.0603	0.130	0.216	0.259	0.190	0.112	0.0239	
	1245.7	3.908	1.464		0.0080	0.0484	0.116	0.206	0.268	0.211	0.116	0.0269	
	1295.5	3.984	1.519		0.0075	0.0507	0.112	0.196	0.256	0.208	0.130	0.0400	
	1345.4	4.112	1.505		0.0065	0.0410	0.100	0.187	0.254	0.222	0.142	0.0473	
	1395.3	4.224	1.493		0.0055	0.0365	0.0882	0.174	0.250	0.240	0.151	0.0545	
$^{55}_{25}Mn$	1160.1	3.640	1.523		0.0085	0.0759	0.157	0.216	0.251	0.178	0.0817	0.0308	
	1265.5	3.772	1.514		0.0076	0.0632	0.139	0.211	0.259	0.195	0.0922	0.0286	0.004 07
	1371.0	3.961	1.539		0.0073	0.0509	0.120	0.198	0.256	0.208	0.115	0.0402	0.005 52

one full unit of charge which is as large as the gas-solid difference $\bar{q}(\mathrm{Al})-\bar{q}_g$ in the region $Z_1\sim 15$. [We note that gas-gas differences in $\bar{q}$ values are small, $\lesssim 10\%$, for target gases Z_2 where $7\leq Z_2\leq 18$ (see Ref. 5)].

Before discussing the large difference, a comment is first necessary regarding gas-solid data. It is well established that the mean charge $\bar{q}_s$ of an ion as observed downstream from a solid target is usually greater than that measured after passage through a gas target $\bar{q}_g$. Betz and Grodzins (BG) (Ref. 6) proposed a model in which the mean charge of the ion inside a solid is the same as in a gas but that substantial multiple excitation occurs inside the solid. The major part of $\Delta\bar{q}=\bar{q}_s-\bar{q}_g$ is then due to Auger transitions after the ions exit from the foil. Baragiola *et al.*[7] examined the Ar→C (thin foil) system by observing the downstream yield of Ar *LMM* Auger electrons. At $v=0.9\ v_0$ where $\bar{q}_s=2.7$,[8] they found that the number of Ar *LMM* Auger electrons per incident projectile N_e^L was 0.24 $\pm$0.03. Since $\bar{q}_g=1.8$ at the same velocity[5] they concluded that N_e^L only accounted for $\sim 25\%$ of $\Delta\bar{q}$, apparently in disagreement with the BG model. Lennard and Phillips[2] attributed the peak observed near $Z_1\sim 15$ in their carbon $\bar{q}$ data to the post-foil Auger decay of projectile *K*- or *L*-shell vacancies; nevertheless, the magnitude of this Auger contribution to $\bar{q}$ was not sufficiently large to explain the solid-gas difference consistent with the observations of Baragiola *et al.*[7]

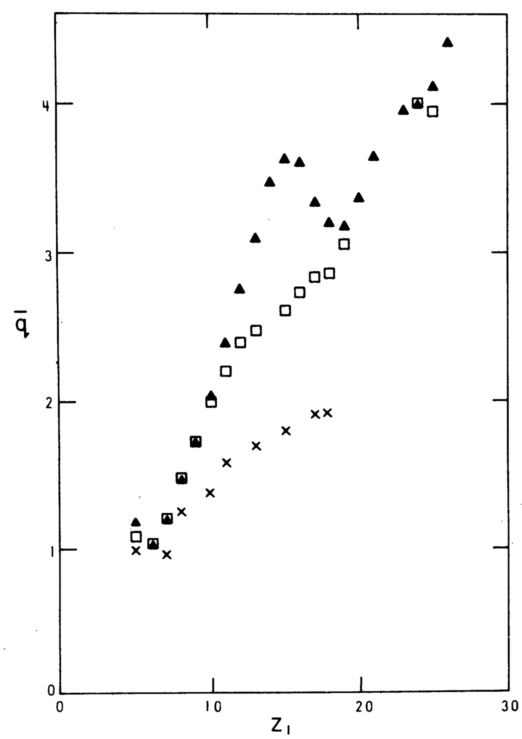

FIG. 1. The open squares show the measured post-foil mean charge $\bar{q}=\sum_q qf_q$ measured for projectiles Z_1 emerging from a thin Al foil. These data are for an exit velocity $v=v_0$. The solid triangles are data for a thin carbon foil (Ref. 2); the crosses are gas-target results ($Z_1\rightarrow N_2$, O_2) from Ref. 5.

To determine whether the solid-solid difference in $\bar{q}$ can be explained on the basis of the difference in Auger *K* or *L* contributions we must examine the corresponding Auger *K*- or *L*-electron yields for projectiles exiting C and Al. For some projectiles Z_1 the Auger *K*-electron yield N_e^K,[9] or Auger *L*-electron yield N_e^L (Ref. 10) per incident projectile after exiting carbon foils is known, see Table II. These values can be used to estimate the maximum contribution $\Delta\bar{q}_A$ of Auger decays to $\bar{q}(\mathrm{C})$. Unfortunately, only the Auger yield for *S* exiting an Al foil is known, $N_e^L=0.11$.[10] This result must be considered an upper limit since no UHV precautions were taken to control the target surface condition. Our estimate from the x-ray data of Feldman *et al.*[11] is that N_e^L for Ar ions exiting an Al foil at $v=v_0$ is $\sim 1/6$ that for carbon foils, i.e., $N_e^L\simeq 0.04$.

The residual values of the mean charges after subtracting the known Auger contributions, $\bar{q}_r=\bar{q}-\Delta\bar{q}_A$, are plotted for both C and Al in Fig. 2 for an exit velocity $v=v_0$. The Auger contribution to $\bar{q}(\mathrm{C})$, while substantial in some cases, does not yield agreement between $\bar{q}_r(\mathrm{Al})$ and $\bar{q}_r(\mathrm{C})$. Except for $Z_1=16$ and 18, no corrections for Auger contributions have been made to the $\bar{q}(\mathrm{Al})$ data of Fig. 2. The corrections would, of course, only in-

TABLE 2. Auger electron yields per incident projectile measured for projectiles emerging from thin carbon foils at $v=v_0$. N_e^K are from Ref. 9; N_e^L are preliminary data (Ref. 10). The uncertainties in N_e^K, N_e^L are $\sim 30\%$.

Z_1	N_e^K	N_e^L
5	0.19	
6	0.035	
7	0.013	
8	0.0025	
13		0.30
14		0.68
15		0.63
16		0.45
18		0.25

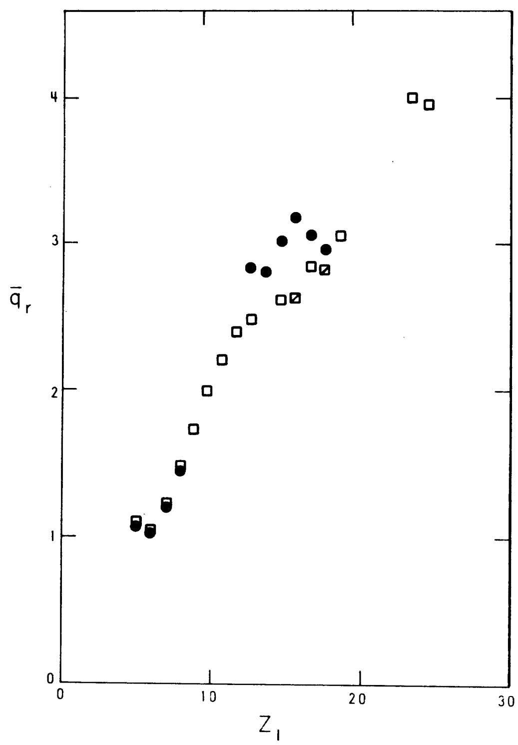

FIG. 2. Residual mean charge $\bar{q}_r = \bar{q} - \Delta\bar{q}_A$ for projectiles Z_1 emerging from C (●) and Al (□ or ▨) foils. For the carbon data, $\Delta\bar{q}_A$ are taken from Table II. For Al, $\Delta\bar{q}_A$ is known for $Z_1 = 16$ and 18 (▨) but for all other Al target data $\Delta\bar{q}_A = 0$ has been assumed and these latter Al data are plotted with a different symbol (□).

crease the differences between the $\bar{q}_r$ values for C and Al.

However, the above interpretations of the gas-solid or solid-solid results using the BG model assumes that the state of excitation of the projectiles within the foil is such that there are no electrons in the N shell. Hartree-Fock calculations of the relevant multiply excited configurations for projectiles in C or Al (such as the calculations of Betz[12] for Br projectiles traversing C) do not exist. A simple estimate based on the criteria of Betz[12] indicates that Ar N shells are meaningful within a solid in the projectile velocity range $v \sim v_0$, and that post-foil Auger decay of such multiply excited states would then yield Ar M Auger electrons N_e^M in number. These low-energy electrons would not have been observed by Baragiola *et al.*[7] There remains the possibility that Auger M-electron yields could account for part or all of the remaining gas-solid difference; however, solid-solid differences are unlikely to be substantially altered by this process.

In summary, we have measured charge-state distributions and derived $\bar{q}$ values for 16 different projectiles incident at low velocities on thin aluminum foils. The dependence of $\bar{q}$ on Z_1 is much stronger than is observed for gas data and is significantly different from that found for C foils. This difference can be as large as that for gas-solid measurements. The contribution to $\bar{q}$ due to Auger K- and L-electron yields measured downstream of C foils is insufficient to bring about agreement between $\bar{q}_r$(C) and $\bar{q}_r$(Al). We conclude that solid-solid differences in $\bar{q}$ are real, large, and at present unexplained. Any description of low-velocity $\bar{q}$ data by semiempirical expressions that are Z_2 independent should therefore be used with caution.

We gratefully acknowledge the contributions of G. A. Sims and D. A. S. Walker to this work. We also thank D. Schneider for making available results in advance of publication.

1. H. D. Betz, Rev. Mod. Phys. 44, 465 (1972).
2. W. N. Lennard and D. Phillips, Phys. Rev. Lett. 45, 176 (1980).
3. W. N. Lennard, D. Phillips, and D. A. S. Walker, Nucl. Instrum. Methods 179, 413 (1981).
4. W. N. Lennard, T. E. Jackman, and D. Phillips, Phys. Lett. 79A, 309 (1980).
5. A. B. Wittkower and H. D. Betz, At. Data 5, 113 (1973).
6. H. D. Betz and L. Grodzins, Phys. Rev. Lett. 25, 211 (1970).
7. R. A. Baragiola, P. Ziem, and N. Stolterfoht, J. Phys. B 9, L447 (1975).
8. W. C. Turkenburg, B. G. Colenbrander, H. H. Kersten, and F. W. Saris, Surf. Sci. 47, 272 (1975).
9. D. Schneider, N. Stolterfoht, D. Ridder, H. C. Werner, R. J. Fortner, and D. L. Matthews, IEEE Trans. Nucl. Sci. NS-26, 1136 (1979).
10. D. Schneider (private communication).
11. L. C. Feldman, R. J. Silverman, and R. J. Fortner, Nucl. Instrum. Methods 132, 29 (1976).
12. H.-D. Betz, Nucl. Instrum. Methods 132, 19 (1976).